Hindawi
Geofluids
Volume 2022, Article ID 1094281, 11 pages
https://doi.org/10.1155/2022/1094281

Research Article

A Study on Excavation Characteristics of Tunnel with Upper-Soft Lower-Hard Stratum

Jun Feng,[1,2] **Hui-juan Yang**,[1] **and Yu Zhang**[3]

[1]*School of Airport Engineering, Civil Aviation Flight University of China, Guanghan 618307, China*
[2]*Engineering Research Center of Airport, CAAC, Beijing 100621, China*
[3]*Department of Coast Defense Engineering, Naval Logistics Academy, Tianjin 300450, China*

Correspondence should be addressed to Jun Feng; sckid1987@163.com

Received 30 May 2022; Revised 15 August 2022; Accepted 3 September 2022; Published 23 September 2022

Academic Editor: Zhengzheng Xie

In view of the geological environment, in which the upper part is the "soft" layer of completely weathered siliceous rock and the lower part is the "hard" layer of weakly weathered limestone, the rail surface line is designed to pass through the interface between the upper "soft" layer and lower "hard" layer. First, the MIDAS/GTS software was used to comprehensively simulate the stress and deformation law of surrounded rock under three excavation methods, which are the positive benching and retaining core soil method, CRD method, and double side drift method, for selecting the appropriate excavation method. After the excavation method was determined, the rule of change in the stress and deformation of the surrounded rock with time in the actual excavation process was analyzed by field monitoring means. Finally, on the basis of the findings in the numerical analysis as well as the field monitoring, the engineering characteristics, such as the stress and deformation of the surrounded rock during the excavation of deep buried tunnels in the upper-soft lower-hard ground, were analyzed. The results revealed the following: (1) Under all three excavation methods, the tunnel deformation was small and met the requirements for tunnel deformation control. (2) Due to the different excavation support sequence, the distribution of lining bending moment of the three excavation methods was widely different. The bending moment of the lining produced by the positive benching method was far less than that of the other two methods. (3) Due to the difference in lithology, the stress of the tunnel lining in the thick upper "soft" and "hard" strata was mainly concentrated on the upper soft rock area, while the stress in the lower hard rock area was relatively small, and the lining stress value generated using the three excavation methods was relatively large. In general, the deformation and stress in the positive benching method construction were less than those in the other two methods. In addition, the positive benching method was convenient for mechanized operation, the construction progress was fast, and the cost was relatively low. Therefore, the positive benching and retaining core soil method is adoptable for this kind of tunnel. (4) The measured stress and deformation at the rail surface line exhibited a change law of first increase, and subsequently, this tended to be stable. The change in stress-time can be expressed by the Boltzmann function, and the change in deformation with time can be well expressed by exponential functions. (5) The stress value and deformation value detected in the actual excavation were greater than the results of the theoretical numerical analysis. However, the findings in the theoretical numerical analysis still have certain guiding significance for actual excavation.

1. Introduction

Tunnel excavation is often faced with complex engineering geological environments. In view of specific geological conditions, selecting the appropriate excavation method is the premise to ensure the safety of tunnel construction [1, 2]. In mountain tunnel engineering, due to the limitation of geological conditions, the line may be selected at the interface between soil and rock. At the soil-rock interface, the overlying soil layer or weathered layer is "soft," and the underlying bedrock is "hard." This makes the tunnel pass through a kind of "upper soft and lower hard" stratum. When crossing this kind of stratum, the safety of the tunnel lining and surrounded rock will be greatly threatened due to the great difference in lithology engineering characteristics between the layers above and beneath the tunnel. Therefore,

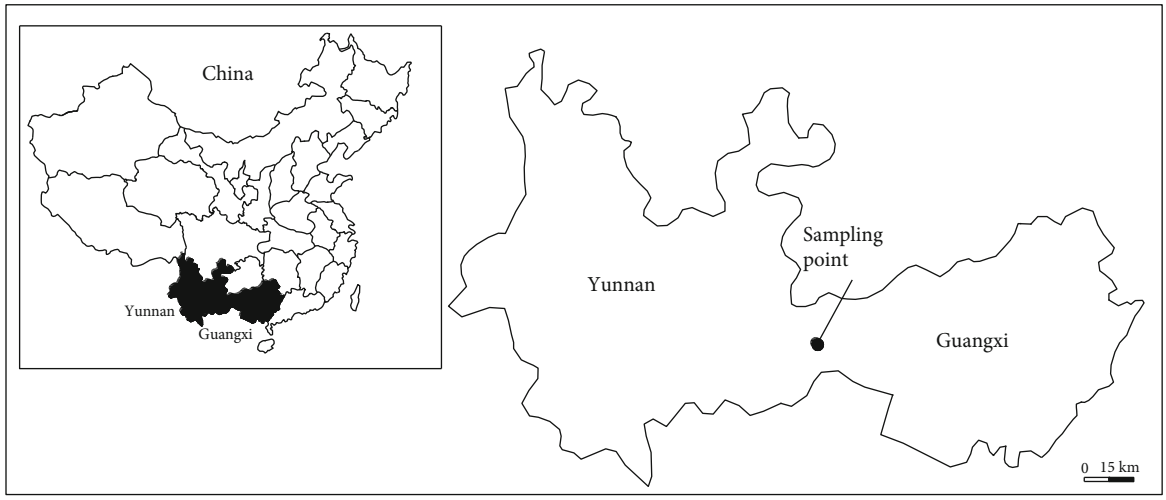

Figure 1: Tunnel location and sampling points.

Figure 2: Rock core of the upper "soft" completely weathered siliceous rock.

Figure 3: Rock core of the lower "hard" moderately weathered limestone.

the selection of the excavation method is crucial. At present, there are many researches on the stress and deformation of surrounded rocks in the process of tunnel construction and excavation, at home and abroad, but there are few studies on tunnel engineering in the "upper soft and lower hard" strata. Li et al. studied the grouting effect on rock fracture based on the shear and seepage assessment [3, 4]. Ding investigated the stress and strain characteristics of different construction methods for tunnels that cross the soil-rock interface stratum and carried out comparisons among schemes [5]. Xie et al. investigated the stress of the tunnel support structure in the upper soft and lower hard strata [6]. Wang and Yang also conducted relevant researches on tunnels in the upper soft and lower hard strata from other angles [7]. Aim at a test tunnel was excavated at the Mont Terri underground rock laboratory (URL) as part of a long-term research project; Lisjak et al. studied the thermo-hydro-mechanical (THM) effects generated by the existence of an underground repository, and the change of stress and strain depended on the time [8]. Causse et al. focused on different mechanisms of slope instability in tunnel excavation. It analyzed the change of stress and strain at different times during the processes of tunneling excavation through numerical simulations [9]. According to Lane Boyd et al., they applied a variogram-based geostatistical algorithm with both borehole data and face maps from the completed Caldecott Tunnel in California, for predicting the anticipated tunneling conditions and associated uncertainty both prior to and during excavation for an integration of the information obtained at various times during the whole life of the project, and an analysis was performed as to the variation of stress and strain with time [10].

In view of these present researches, there are few studies on the choice of the construction methods and the variation law of stress and deformation with time during excavation. In most of these researches, the overlying "soft" layer is less than 100 m, which can include most of the strata encountered in practice [11–16]. However, due to the particularity of engineering geology, the situation that the overlying "soft" layer reaches or even exceeds 100 m would be encountered in practice, and there are few studies on this type of "deep buried" tunnel, at present. In addition, in this geological condition, the variation law of surrounded rock stress and strain with time will have an important impact on the safety of tunnel construction, and its subsequent operation. The Guiqing tunnel between Yunnan and Guangxi is an important channel to connect the two provinces. The overlying stratum of the tunnel is a completely weathered siliceous rock layer with a thickness of nearly 100 m; the underlying

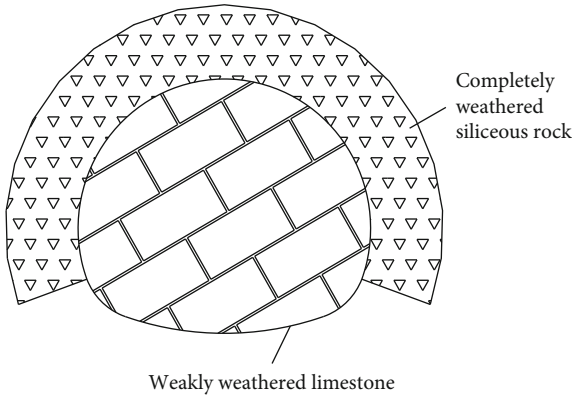

Figure 4: Diagram of the typical tunnel face.

bedrock is limestone, which is a "hard" layer. Due to the limitation of geological conditions, in design, the route of the tunnel just passes through the interface of the soft part and hard part. For this kind of "deep buried" mountain tunnel that passes through an upper-soft lower-hard layer, the analysis of the deformation characteristics of surrounded rock during excavation is of great guiding significance to the selecting the excavation method, design, and construction of similar projects.

2. Tunnel Overview

2.1. Project Location. The Guiqing tunnel crosses Yunnan and Guangxi. Before carrying out relevant researches, the representative sections were selected for sampling, according to the characteristics of the regional geological environment, and relevant laboratory tests are carried out for obtaining the basic physical and mechanical parameters in terms of the upper "soft" and lower "hard" layers. For the sampling points, please refer to Figure 1.

2.2. Geological Conditions. The upper part of the tunnel passes through the siliceous rocks of the upper Permian System Heshan formation (P_2h), which is completely weathered. The original rock structures are basically damaged, and some residual parts are still visible, presenting with a hard plastic shape. The drilling revealed that the rock core looks like soil with 30% fine breccia, and the particle size was 0.5-20 mm, as shown in Figure 2. The lower part passes through the limestone of the lower Permian system Maokou Formation (P_1m), which is calcareous cemented, with a medium thick to thick layered structure. The rock mass was relatively complete, hard, and brittle, as shown in Figure 3. The tunnel cavern was located at the interface, between the completely weathered siliceous rock layer and limestone. The completely weathered siliceous rock layer was approximately 100 m thick. For a typical face, please refer to Figure 4.

The tunnel body was located in the seasonal variation zone of the underground karst water. The groundwater was mainly fissure water and karst pipeline water with strong water yield, and water and mud inrush may be encountered during construction. Especially in rainy season, it would be easy to encounter underground pipeline water gushing.

2.3. Design Parameters. For the basic physical and mechanical parameters for the upper "soft" formation and lower "hard" formation, please refer to Tables 1 and 2, respectively. The physical properties and mechanical parameters of the "soft" layer were obtained by laboratory test with representative samples before simulation. For the physical properties and mechanical parameters of the "hard" layer, one aspect depends on the laboratory test results of representative samples in the field, and the other aspect depends on the test results of point loads in the field.

3. Numerical Analysis of Different Construction Methods

In order to analyze the stress and deformation characteristics of the surrounded rock under various excavation methods, based on the construction principle of NATM, the positive benching and retaining core soil method, CRD method, and double side drift method were adopted. In order to analyze the applicability of these methods, the Midas/GTS numerical analysis software was selected for making a numerical analysis.

3.1. Modeling and Meshing. According to the section size, support parameters, and stratum distribution, a two-dimensional plane model was established, as shown in Figure 5. Taking 50 m from the left, right, and downward sides of the model, respectively, the thickness of overburden layer was 100 m at the top of the model. The material of the surrounded rock was the 2D plane element, the constitutive model was the Mohr Coulomb model, the 1D element of concrete and rock bolt was the linear element, and the constitutive model was the linear elastic model. The secondary lining is not considered the safety reserve.

In order to adapt to the three different excavation methods, combined with the characteristics of the MIDAS/GTS software, the square grid was adopted for the positive benching and retaining core soil method, and the triangular grid was adopted when using the CRD method and double side drift method. The grid meshing is as indicated in Figure 5.

3.2. Parameter Selection. The upper "soft" layer and the lower "hard" layer were modeled based on the parameters in Tables 1 and 2. At the same time, combined with the actual engineering support mode, the support parameters in Table 3 were selected for the analysis.

3.3. Result Analysis

3.3.1. Variation Characteristics of Vertical Displacement. The vertical displacement variation characteristics of the tunnel surrounded rock caused by the three excavation methods are shown in Figure 6.

It can be observed from Figure 6 that the maximum displacement in the vertical level in the case of the use of the positive benching method and double side drift method

Table 1: Basic physical and mechanical parameters for the upper "soft" formation.

Physical and hydraulic property index											Natural quick shear		Coefficient of compressibility	Modulus of compressibility	Coefficient of consolidation	Osmotic coefficient
Natural density	Grain density	Natural moisture content	Natural void ratio	Porosity	Liquid limit (10 mm)	Plastic limit	Plasticity index	Liquidity index	Dry density	Free swell ratio	Cohesion	Internal friction angle	a_v	Es (v)	C_v	Kv
ρ	ρ_S	ω	e	n	W_L	Wp	I_p	I_L	ρ_d	Fs	c	φ		(100~200) kPa		
(g/cm^3)	(g/cm^3)	(%)		(%)	(%)	(%)			(g/cm^3)	(%)	(kPa)	(°)	MPa^{-1}	MPa	$(cm^2/s) \times 10^{-3}$	$(cm/s) \times 10^{-8}$
1.92	2.74	32.5	0.891	47.1	55.8	26.3	29.5	0.2	1.45	41	34.0	16.3	0.47	2.93	2.939	7.481

Table 2: Basic physical and mechanical parameters for the lower "hard" formation.

Sampling depth	Rate of weathering	Bulk density	Grain density	Compressive strength		Internal friction angle	Cohesion	Elasticity modulus	Poisson's ratio
				Nature	Saturation				
h (m)		ρ_S' (g/cm^3)	ρ_S'' (g/cm^3)	$\sigma_{S\text{-nature}}$ (MPa)	$\sigma_{S\text{-saturated}}$ (MPa)	φ' (°)	c' (kPa)	E (GPa)	v
97.5~102.5	Weakly weathered	2.75	2.79	49.9	46.85	42	45	11.6	0.3

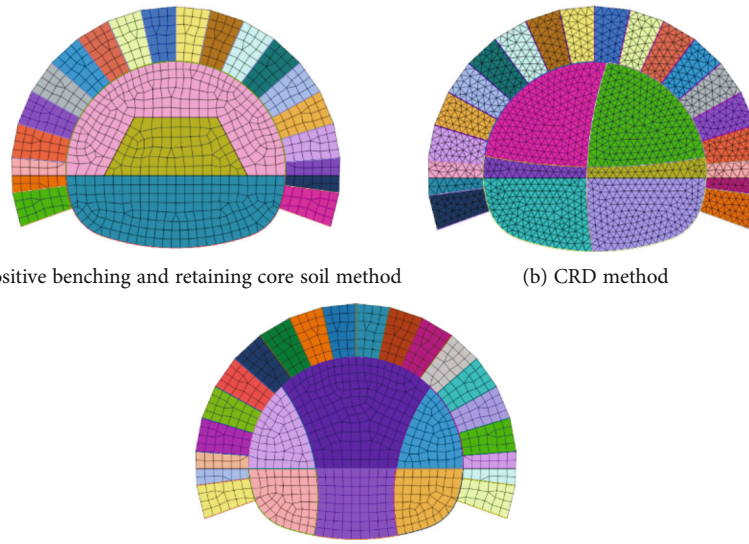

(a) Positive benching and retaining core soil method (b) CRD method

(c) Double side drift method

Figure 5: Modeling and meshing.

Table 3: Material characteristic parameters.

Material	Unit weight (kN/m^3)	Elasticity modulus (GPa)	Poisson's ratio	Internal friction angle (°)	Cohesion (kN/m^2)
C20 spray concrete	22.0	21.00	0.2	/	/
Rock bolt	78.0	200.00	0.3	/	/

was used 13.7 mm and 14.4 mm, respectively, and these were located at the vault of the tunnel. The maximum displacement in the vertical level in the case of the use of the CRD method was 16.3 mm and was located on the right side of the arch crown. All of these met the requirements for deformation control in the design of the railway tunnel.

In the CRD method, for the adaptability of matching software, triangular mesh is adopted, which is more detailed. Therefore, the results obtained are different from the other two methods, showing that there is a peak deformation value on both the left and right sides of the vault, but it can be seen that the maximum value appears in the right vault.

3.3.2. Bending Moment Variation Characteristics. The bending moment variation of the lining in these three excavation methods is shown in Figure 7.

It can be observed from Figure 7 that the maximum bending moments of the three excavation methods are 65.4 kN·m, 186.3 kN·m, and 139.3 kN·m, respectively. It can be observed that the bending moment in the case of the use of the CRD method was the largest, and the bending moment caused by the positive benching method was far less than the other two methods. Due to the different excavation methods, the distribution of lining moment was significantly different. The maximum bending moment for the positive benching method was located at the interface of the soft and hard layers, and the lining in the soft rock area and hard rock area could both bear the maximum bending moment. The maximum bending moment caused by the CRD method was located in the upper part of the interface, between the soft and hard layers, and the bending moment of the left and right lining was asymmetric distributed. The maximum

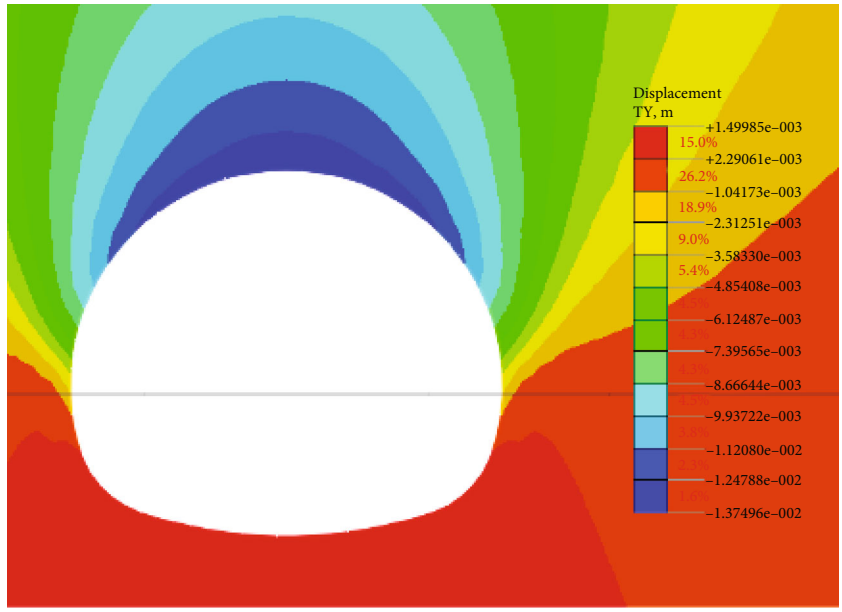

(a) Positive benching and retaining core soil method

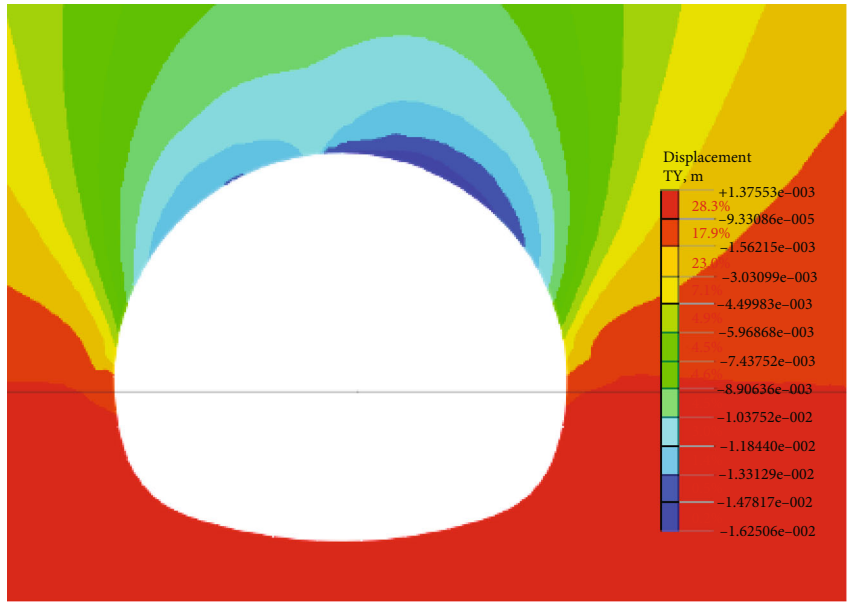

(b) CRD method

Figure 6: Continued.

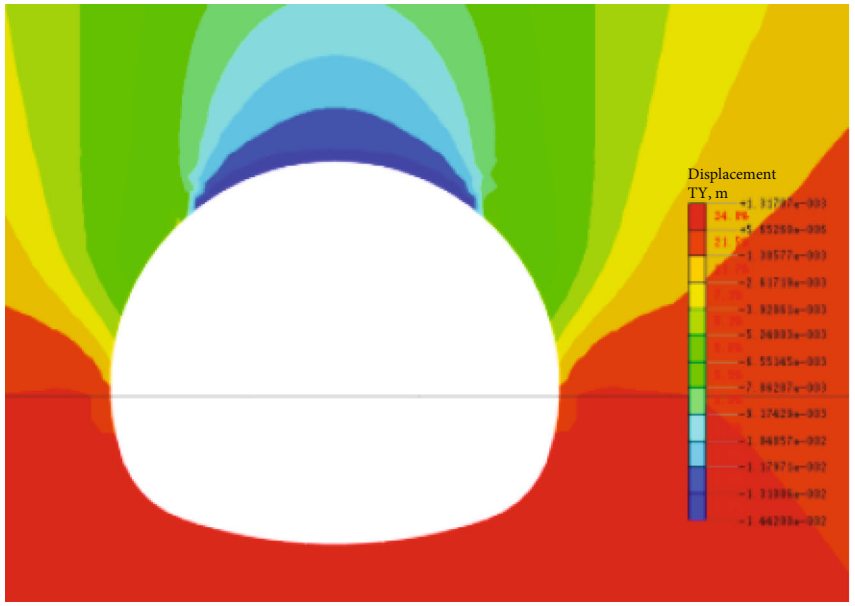

(c) Double side drift method

Figure 6: The vertical displacement variation characteristics.

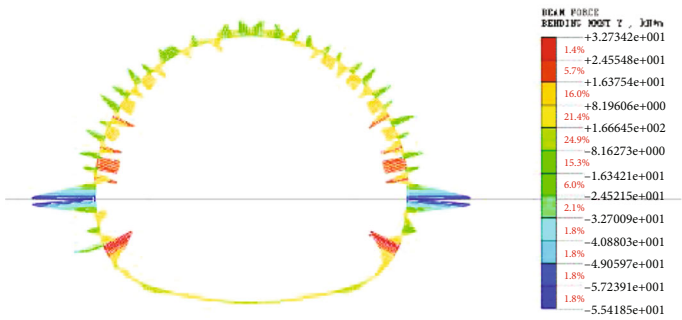

(a) Positive benching and retaining core soil method

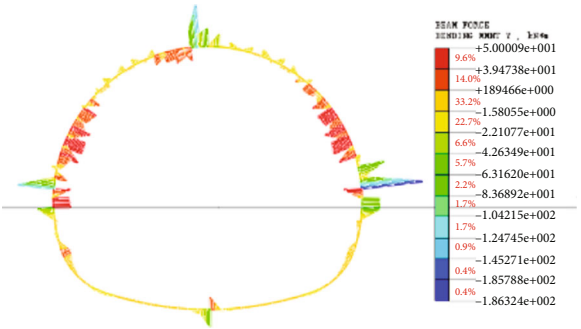

(b) CRD method

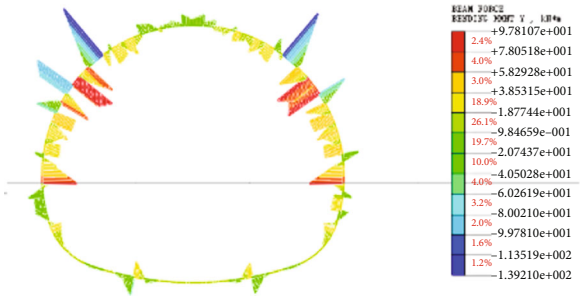

(c) Double side drift method

Figure 7: Bending moment variation characteristics.

bending moment in the case of the use of the double side drift method was located at the arch shoulder. Because the core soil is reserved in the excavation of CRD method, each step of the excavation is sealed into a ring, which has the advantages of the other two methods. Therefore, the effect of the reserved core soil was considered in the simulation, and it was difficult to show the symmetry of the left and right bending moments in the simulation as in the other two methods, resulting in local asymmetry of the left and right bending moments in the results.

3.3.3. Variation Characteristics of Axial Force. The axial force variation of the lining for the three excavation methods is shown in Figure 8.

As indicated in Figure 8, in terms of the axial force, the tunnel lining in the deep buried soil rock interface stratum

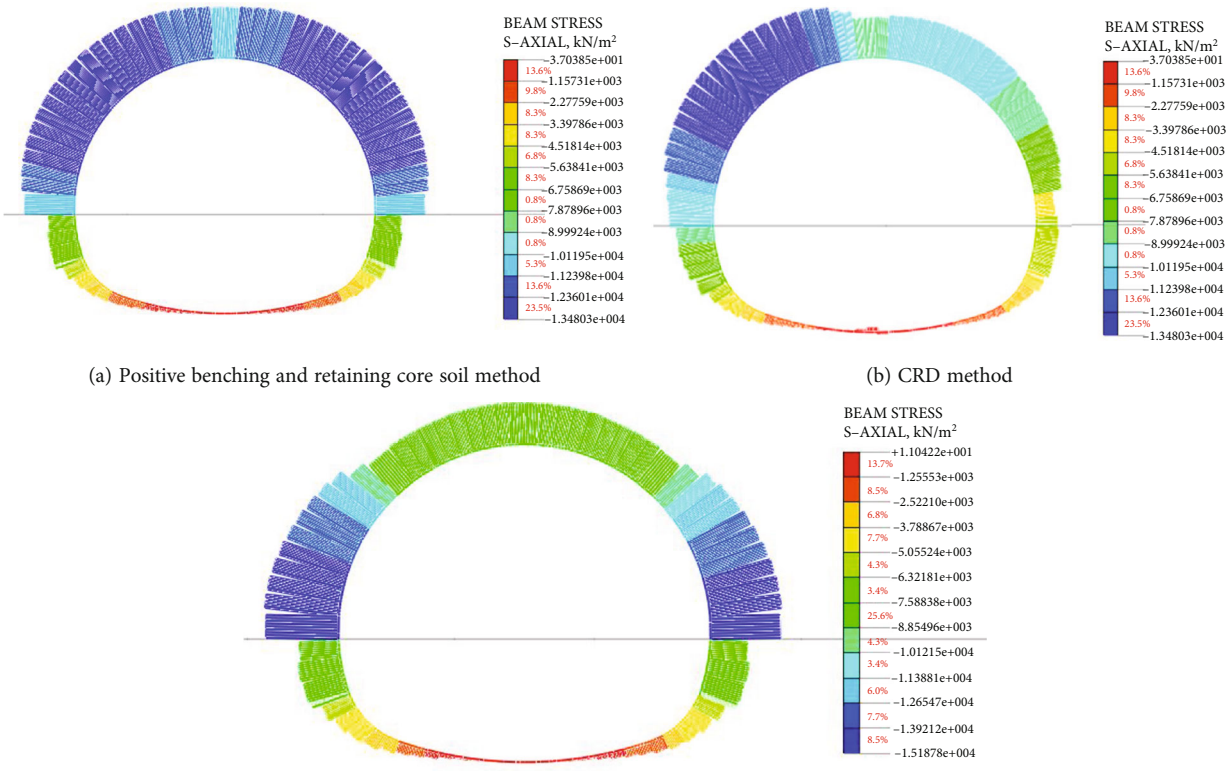

(a) Positive benching and retaining core soil method

(b) CRD method

(c) Double side drift method

Figure 8: Variation characteristics of axial force.

Figure 9: Sensor for stress monitoring.

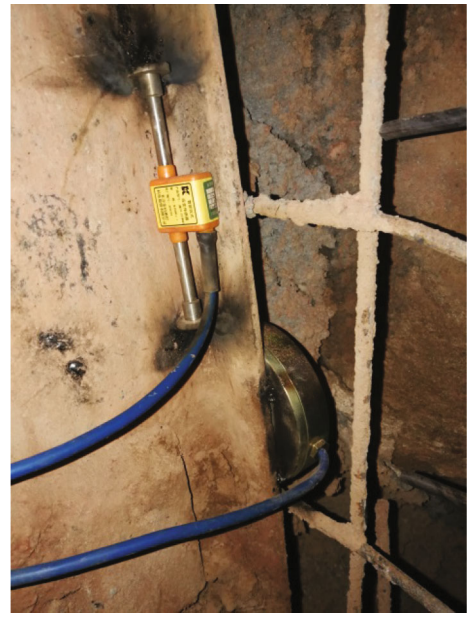

Figure 10: Sensor for deformation monitoring.

was mainly distributed in the upper part, that is, the completely weathered siliceous rock layer. Among these, the maximum support stress in the case of using the positive benching method was 13.5 MPa, the maximum support stress when the CRD excavation method was adopted was 13.9 MPa, and the maximum support stress when the double side drift method was applied was 15.2 MPa. The stress value under these three methods was all large. The stress had a value, under the double side drift method, close to the ultimate compressive strength of C20 concrete, which is 15.5 MPa. Because the core soil is reserved in the excavation of CRD method, each step of the excavation is sealed into a ring, the effect of the reserved core soil was considered in the

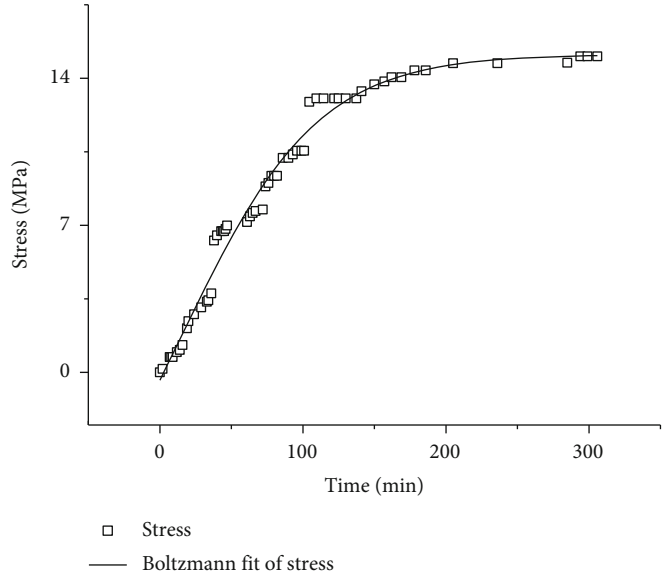

Figure 11: Stress curve for the rail surface line with time.

simulation, and the axial force with the CRD excavation method is deflected compared to the other two methods.

4. On-Site Monitoring

Combined with the findings in the numerical analysis, the positive benching method was selected in the actual construction. For a verification of the numerical analysis in terms of the rationality, before the construction and excavation, the representative section was selected to be embedded with the relevant stress and deformation monitoring equipment. Combined with the findings in the field monitoring and numerical analysis, the stress and deformation mechanism of the tunnel in the excavation process was comprehensively analyzed.

4.1. Burying Monitoring Equipment. In order to compare with the results of the numerical analysis, representative sections were selected before the tunnel excavation, and stress and deformation monitoring equipment are embedded in the interface of the upper "soft" and "hard" layers, namely, the arch side and the crown of the rail surface line, as shown in Figures 9 and 10. With the progress of the excavation, the changes in stress and deformation with time were recorded.

4.2. Monitoring Results and Prediction. According to the statistics for the change in stress and deformation with time, the change curve for stress with time was obtained, as shown in Figure 11.

It can be observed from Figure 11 that with the construction and excavation, the stress at the rail surface line initially increased and subsequently tended to be stable, and this can be well expressed by the Boltzmann function. The change mechanism was analyzed, as follows: before the construction and excavation, the stress was in the state of equilibrium and stability in all directions; after the construction and excavation started, the stress in the upper "soft" and "hard" layers

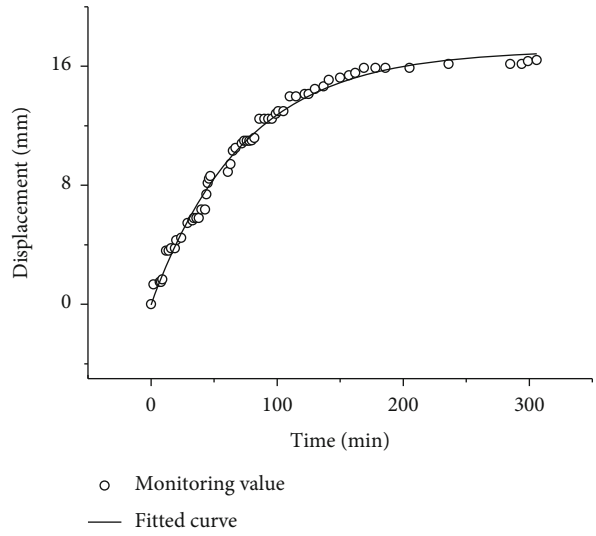

Figure 12: The curve for the rail surface deformation with time.

was released, and stress redistribution rapidly occurred, which gradually tended to a new state of stress balance with the excavation. As indicated in the figure, after 300 minutes of excavation, the stress basically tended to be stable, and the stable value is approximately 14.40 MPa.

The curve of the deformation at the rail surface with time is shown in Figure 12.

It can be observed from Figure 12 that with the construction and excavation, the deformation at the rail surface line initially increased and subsequently tended to be stable, which can be well-expressed by exponential functions. The change mechanism was analyzed, as follows: before the construction and excavation, the two kinds of strata are not disturbed, and the rail surface line was in a stable state of deformation coordination; after the construction and excavation started, the deformation of the upper "soft" and lower

Table 4: Comparison of stress at the rail surface line.

Research method		
Numerical analysis	Field monitoring	Difference rate
13.50	14.40	6.25%

Maximum stress (MPa).

Table 5: Comparison of deformation at the rail surface line.

Research method		
Numerical analysis	Field monitoring	Difference rate
13.70	16.01	14.43%

Maximum deformation (mm).

"hard" layers was different and discordant due to the difference in strata, but with the passage of excavation time, the deformation adjustment of these two layers at the interface would continue to occur, and finally, the deformation would be harmonious and consistent, and the deformation would tend to be stable at the rail surface line. It can be observed from the figure that the deformation tended to be stable after 300 minutes of excavation, with a stable value of approximately 16.01 mm.

4.3. Comparisons of Results. As per the numerical analysis findings as well as field monitoring, the comparison of stress and deformation at the rail surface line after turning into stability under the positive benching method can be obtained, as shown in Tables 4 and 5.

It can be observed from Table 4 that the actual excavation monitoring stress value was greater than the theoretical numerical analysis result. Due to the influence of comprehensive external factors, such as construction disturbance on the tunnel engineering, the stress value of the upper "soft" layer was initially released and redistributed, while the response of the lower "hard" layer was relatively slow. Hence, the measured stress value would be slightly larger than the theoretical value. However, the difference rate was 6.25%, which was not more than 10%. Therefore, the results of the numerical analysis still have a certain theoretical guiding significance for the actual excavation.

It can be observed from Table 5 that the deformation value of the actual excavation monitoring was greater than that of the theoretical numerical analysis. Due to the influence of comprehensive external factors, such as construction disturbance during the actual excavation process of tunnel engineering; the "soft" layer on the upper part of the tunnel face was initially subjected to strong deformation, which does not completely occur, in accordance with the change trend of the theoretical analysis. At the same time, after the deformation was coordinated and stable, the value also changed with the change in the lower "hard" layer. Hence, the measured deformation value would be greater than the theoretical value, and the difference rate was found to be 14.43%, which is not more than 15%. Therefore, the results of the numerical theoretical analysis still have certain theoretical guiding significance for the actual excavation.

5. Conclusions

In view of the stratum with the "soft" layer of completely weathered siliceous rock in the upper part and the "hard" layer of weakly weathered limestone in the lower part, a deep buried tunnel project with the rail surface line passing through the interface between the upper "soft" layer and the lower "hard" layer was designed. By means of theoretical numerical analysis and field monitoring, the variation law of stress and deformation at the rail surface line with construction time was comprehensively analyzed, and we had the below conclusions:

(1) The deformation of the tunnel caused by the three excavation methods was small, which meets the requirements for tunnel deformation control. Due to the different support sequences, the distribution of the lining bending moment caused by the three excavation methods was widely different. The bending moment produced by the positive benching method was significantly lesser than that of the other two methods. The deformation and stress for the positive benching method are less than those for the other two methods. Furthermore, the positive benching method is convenient for mechanized operation, the construction progress is fast, and the cost is relatively low. Therefore, the positive benching and retaining core soil method should be adopted for this kind of tunnel

(2) The results showed that the stress and deformation at the rail surface line initially increased and subsequently tended to be stable. The change in stress-time can be well expressed by the Boltzmann function, and the maximum stable value is approximately 14.40 MPa. The change in deformation with time can be well expressed by exponential functions, and the maximum stable value is approximately 16.01 mm

(3) The stress value and deformation value monitored in the actual excavation were greater than the results of the theoretical numerical analysis. The difference rate of the stress value was 6.25%, which was not more than 10%, while the difference rate of the deformation value was 14.43%, which was not more than 15%. The results of the numerical analysis still have a certain theoretical guiding significance for the actual excavation

Data Availability

The data were obtained by experiments, and the simulation was carried out by professional software.

Conflicts of Interest

The authors declare that there are no conflicts of interest regarding the publication of this article.

Acknowledgments

This paper was financially supported by the Natural Science Foundation of Sichuan Province (Project No. 2022NSFSC0999), the Fundamental Research Funds for the Central Universities (Project No. J2022-038), the 2021 Open Project of Failure Mechanics and Engineering Disaster Prevention, Key Lab of Sichuan Province (No. FMEDP202110), and a grant from the Engineering Research Center of Airport, CAAC (No. ERCAOTP20220302).

References

[1] Z. Diao and J. Li, "Study on construction of large section tunnels in upper soft and lower hard layers," *Tunnel Construction*, vol. S2, pp. 433–436, 2007.

[2] Q. Meng, H. Wang, M. Cai, W. Xu, X. Zhuang, and T. Rabczuk, "Three-dimensional mesoscale computational modeling of soil-rock mixtures with concave particles," *Engineering Geology*, vol. 277, article 105802, 2020.

[3] Z. Li, H. Liu, Z. Dun, L. Ren, and J. Fang, "Grouting effect on rock fracture using shear and seepage assessment," *Construction and Building Materials*, vol. 242, article 118131, 2020.

[4] Z. Li, S. Liu, W. Ren, J. Fang, Q. Zhu, and Z. Dun, "Multiscale laboratory study and numerical analysis of water-weaken\ing effect on shale," *Advances in Materials Science and Engineering*, vol. 2020, Article ID 5263431, 14 pages, 2020.

[5] L. Ding, "Tunnel excavation and supporting scheme selection based on numerical simulation," *Site Investigation Science and Technology*, vol. 3, pp. 9–28, 2012.

[6] Z. Xie, J. He, Y. Shi, and J. Yang, "The internal force of the supporting structure and surrounded rock failure analysis in the bias soil-rock tunnel," *Journal of Geotechnical Investigation & Surveying*, vol. 41, no. 5, pp. 23–27, 2013.

[7] R. Wang and X. Yang, "Rock control on the mined tunnel construction undercrossing through existed building in upper-soft and lower0hard stratum," *Journal of Jiamusi University (Natural Science Edition)*, vol. 32, no. 2, pp. 191–197, 2014.

[8] A. Lisjak, B. Garitte, G. Grasselli, H. R. Müller, and T. Vietor, "The excavation of a circular tunnel in a bedded argillaceous rock (Opalinus Clay): short-term rock mass response and FDEM numerical analysis," *Tunnelling and Underground Space Technology*, vol. 45, pp. 227–248, 2015.

[9] L. Causse, R. Cojean, and J.-A. Fleurisson, "Interaction between tunnel and unstable slope - influence of time-dependent behavior of a tunnel excavation in a deep-seated gravitational slope deformation," *Tunnelling and Underground Space Technology*, vol. 50, pp. 270–281, 2015.

[10] D. Lane Boyd, G. Walton, and W. Trainor-Guitton, "Geostatistical estimation of ground class prior to and during excavation for the Caldecott Tunnel Fourth Bore project," *Tunnelling and Underground Space Technology*, vol. 100, article 103391, 2020.

[11] G. Galli, A. Grimaldi, and A. Leonardi, "Three-dimensional modelling of tunnel excavation and lining," *Computers and Geotechnics*, vol. 31, no. 3, pp. 171–183, 2004.

[12] V. A. Kontogianni and S. C. Stiros, "Induced deformation during tunnel excavation: evidence from geodetic monitoring," *Engineering Geology*, vol. 79, no. 1-2, pp. 115–126, 2005.

[13] N.-A. Do, D. Dias, P. Oreste, and I. Djeran-Maigre, "2D tunnel numerical investigation: the influence of the simplified excavation method on tunnel behaviour," *Geotechnical and Geological Engineering*, vol. 32, no. 1, pp. 43–58, 2014.

[14] X. Li, S.-h. Zhou, H. Di, and P. Wang, "Evaluation and experimental study on the sealant behaviour of double gaskets for shield tunnel lining," *Tunnelling and Underground Space Technology*, vol. 75, pp. 81–89, 2018.

[15] X. Li, H. Di, S. Zhou, P. Huo, and Q. Huang, "Effective method for adjusting the uplifting of shield machine tunneling in upper-soft lower-hard strata," *Tunnelling and Underground Space Technology*, vol. 115, article 104040, 2021.

[16] Y. Wang, Y.-J. Zhang, Z. Zhu, M. Du, and Y. Qi, "A novel method for analyzing the factors influencing ground settlement during shield tunnel construction in upper-soft and lower-hard fissured rock strata considering the coupled hydro-mechanical properties," *Geofluids*, vol. 2020, Article ID 6691157, 13 pages, 2020.